

Multigrid Methods with Newton-Gauss-Seidel Smoothing and Constraint Preserving Interpolation for Obstacle Problems

Chunxiao Wu¹ and Justin W.L. Wan^{2,*}

¹ Centre for Computational Mathematics in Industry and Commerce, University of Waterloo, Waterloo, Ontario, Canada

² David R. Cheriton School of Computer Science and Centre for Computational Mathematics in Industry and Commerce, University of Waterloo, Waterloo, Ontario, Canada

Abstract. In this paper, we propose a multigrid algorithm based on the full approximate scheme for solving the membrane constrained obstacle problems and the minimal surface obstacle problems in the formulations of HJB equations. A Newton-Gauss-Seidel (NGS) method is used as smoother. A Galerkin coarse grid operator is proposed for the membrane constrained obstacle problem. Comparing with standard FAS with the direct discretization coarse grid operator, the FAS with the proposed operator converges faster. A special prolongation operator is used to interpolate functions accurately from the coarse grid to the fine grid at the boundary between the active and inactive sets. We will demonstrate the fast convergence of the proposed multigrid method for solving two model obstacle problems and compare the results with other multigrid methods.

AMS subject classifications: 65M55, 65M22, 65F10, 65F50

Key words: Multigrid method, obstacle problem, elliptic variational inequality, complementarity problem, Hamilton-Jacobi-Bellman equation, full approximation scheme.

1. Introduction

The obstacle problem is to find the equilibrium position of an elastic membrane which is constrained to lie below and/or above some given obstacles. Due to the obstacle constraints, the problem is often posed as a constrained minimization problem [3, 19]. Since the contact location of the membrane and the obstacle is usually unknown, sometimes the obstacle problem is studied as free boundary problem [5]. Obstacle problem can also be formulated as elliptic variational inequalities [8], linear complementarity problems [2, 17], and Hamilton-Jacobi-Bellman (HJB) equations [10]. All these formulations result in a nonlinear problem. A finite difference or finite element discretization will yield a nonlinear

*Corresponding author.

system of discrete equations. This paper considers fast solvers and in particular multigrid methods for solving the nonlinear discrete equations.

Many methods have been introduced to solve elliptic variational inequality partial differential equations (PDEs). Projected relaxation methods are popular techniques to solve elliptic variational inequalities [6, 7]. They are known to be easy to implement and convergent. However, the drawback of this approach is that its convergence depends on the choice of the relaxation parameter and has a slow asymptotic convergence rate.

Various forms of preconditioned conjugate gradient (PCG) algorithms for solving nonlinear variational inequalities are presented in [16]. They are more efficient than the projected relaxation method in some cases. However, the rates of convergence still depend on the size of the problem. For problems with small grid sizes, PCG methods may not be very efficient.

A multigrid method is introduced in [8] to solve the finite difference discretized PDE for an obstacle problem. Two phases are used in this method. The aim of the first phase, in which a sequence of coarse grids is used, is to get a good initial guess for the iterative phase two. In the second phase, the problem is solved by a W-cycle multigrid method. A cutting function is applied after the coarse grid correction. The convergence is shown to be better than PCG. However, the application of the cutting function and the phase one may lead to more expensive computations overall.

Elliptic variational inequalities can be reformulated as linear complementarity problems. A multigrid method, namely, projected full approximate scheme (PFAS), is proposed in [2] to solve linear complementarity problems arising from free boundary problems. The multigrid method is based on the full approximate scheme (FAS), which is often used for solving nonlinear PDEs. The multigrid method is built on a generalization of the projected SOR. Two further algorithms based on PFAS are introduced: PFASMD and PFMG, both of which are faster than PFAS. These methods show better convergence rates than the method in [8].

In [17], a PFAS multigrid is applied to solve the American style option problem which is formulated as a linear complementarity problem. The American style option problem can be viewed as an obstacle type problem where the obstacle is given by the payoff function. An F-cycle multigrid method is applied and a Fourier analysis of a smoother is provided. A comparison between an F-cycle and a V-cycle for solving linear complementarity problems is shown. In general, F-cycles show faster convergence than V-cycles [17]. However, an F-cycle requires more computations in each iteration, and so it is relatively more expensive.

Elliptic variational inequalities can also be reformulated as Hamilton-Jacobi-Bellman (HJB) equations. A multigrid algorithm which involves an outer and an inner iteration is proposed in [10]. The active and inactive sets of all grid levels are computed and stored in the outer loop. A W-cycle FAS multigrid method is applied to solve a linearized PDE in the inner iteration. An iterative step similar to [8] is adopted to compute a good initial guess using a sequence of coarse grids. The computational complexity largely depends on the stopping criterion for the inner loop. If the stopping criterion is not chosen wisely, the total computations can be expensive.

A multilevel domain decomposition and subspace correction algorithm are proposed

in [20] to solve the nonlinear variational inequalities for obstacle problems. A special interpolation operator is introduced for decomposing the functions. A proof of the linear rate of convergence for the proposed algorithms is provided.

A so-called monotone multigrid method and a truncated version are introduced in [13] to solve the obstacle problem formulated as elliptic variational inequalities. It has been reported that the convergence rate of the proposed method demonstrates similar convergence as for the classical multigrid for the unconstrained case.

We also remark that semi-smooth Newton methods have been proposed and analyzed for solving constrained variational problems in infinite dimensions (or function space); for example [9, 12]. The variational problem is usually written as a primal-dual system. This approach is similar to the HJB approach in that they both involve the max (or min) operator. However, in the HJB approach, the dual variable is not considered explicitly.

In this paper, we will consider two kinds of obstacle problems. They share the same boundary conditions and obstacle constraints, but with different partial differential operators: one is with the Laplacian operator, and the other is related to the minimal surface operator. We will propose an efficient multigrid method for solving the discrete equations arising from the obstacle problems.

The contributions of the paper are summarized as follows:

- The proposed multigrid method solves both the elastic membrane and minimal surface obstacle problems in the HJB formulation.
- We use a modified version of the Newton-Gauss-Seidel (NGS) method, which is based on a nonsmooth Newton's method, as smoother for multigrid.
- Instead of linear interpolation, we use a constraint preserving prolongation for interpolating coarse grid functions to the fine grid.
- In standard FAS, the coarse grid operators are typically constructed by direct discretization. We use the Galerkin coarse grid operator instead for the elastic membrane constrained obstacle problem.

More detailed descriptions of the method will be given in the later sections. Here we briefly explain the motivation or ideas of the techniques used. The HJB formulation captures the variational inequalities associated with the obstacle problem by the max or min operators. On the one hand, the max and min operators are convex functions, which tend to show nice numerical behaviour. On the other hand, they are not smooth and hence standard nonlinear solvers such as Newton do not work. A nonsmooth version of the Newton's method is required. One challenge of the obstacle problem is the obstacle constraint. Linear interpolation, in general, does not preserve the obstacle constraint, which may lead to inaccurate coarse grid correction. It is desirable to preserve the constraint explicitly. Finally, a Galerkin coarse operator is often used for solving linear problems but seldom used in nonlinear problems. We explore this idea for the case of the elastic membrane constrained obstacle problem, and the resulting multigrid method shows better convergence.

This paper is organized as follows: the obstacle problems, their mathematical derivations, and the numerical discretization are given in Section 2. Section 3 presents multigrid methods based on V-cycle FAS to solve the two kinds of obstacle problems. In Section 4, numerical experiments are given to demonstrate the efficiency of the proposed multigrid methods. Finally, concluding remarks are made in Section 5.

2. Obstacle problems

The obstacle problem discussed in the multigrid literature is to find the equilibrium position of a membrane above (or below) an obstacle, with a fixed boundary. The solution to the obstacle problem can be separated into two different regions. One region is where the solution equals the obstacle value, also known as the active set, and the other region is where the solution is above (or below) the obstacle, the inactive set. The interface between the two regions is called the free boundary. So the obstacle problem is sometimes referred as free boundary problem [3]. Figure 1 shows an example of the obstacle (left) and the solution to the obstacle problem (right).

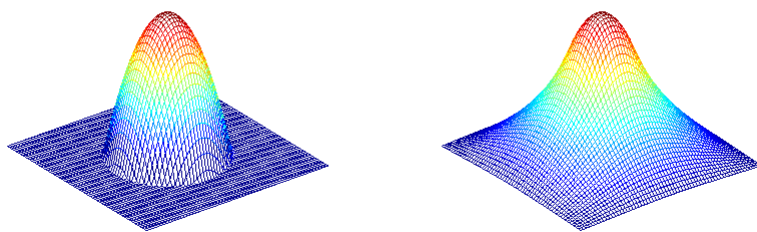


Figure 1: An obstacle problem example, (left) the obstacle, (right) the solution.

In this paper, we will consider two kinds of obstacle problems, which are commonly solved in the multigrid literature. One is based on the classical linear elasticity theory and the other one is based on minimal surface. The two model problems are described in the following sections.

2.1. Elastic Membrane Constrained by an Obstacle

An elastic membrane considered in classical elasticity theory is a thin plate, which has no resistance to bending, but responds only to tension [19]. We assume that a membrane in a domain $\Omega \subset \mathbb{R}^2$ on the 2D plane is equally stretched by a uniform tension, and loaded with the external force f , which is also uniformly distributed. At each point (x, y) on the domain Ω , the displacement is given by $u(x, y)$ which is the unknown function to be

computed. For simplicity, we assume a Dirichlet boundary condition where $u(x, y) = 0$ on the boundary $\partial\Omega$. The obstacle is given by a function $\psi(x, y)$.

An obstacle problem can be classified into one of the three categories based on the position of the obstacle: (a) the lower obstacle problem, in which the solution u lies above the obstacle, (b) the upper obstacle problem, in which the solution u lies below the obstacle, and (c) the two sided obstacle problem, in which the solution u lies in between two obstacles.

In the literature, there are three major formulations of the obstacle problem: elliptic variational inequality, linear complementarity problem, and Hamilton-Jacobi-Bellman (HJB) equation, which are explained below.

Elliptic variational inequality formulation

For now, we consider the lower obstacle problem; i.e. we look for solution u that belongs to the set

$$K = \{u \in H^1 : u \geq \psi\},$$

where H^1 is the standard Sobolev space. The membrane constrained obstacle problem is to find $u \in K$ such that it minimizes the potential energy,

$$\min_v E(v) \equiv \int_{\Omega} \frac{1}{2} |\nabla v|^2 dx dy - \int_{\Omega} f v dx dy, \quad (2.1)$$

where f is an external force. Let u be the solution of (2.1); i.e.

$$E(u) \leq E(v), \quad \forall v \in K. \quad (2.2)$$

Since K is a convex set, $u + \lambda(v - u) \in K$ for $\lambda \in [0, 1]$. Define $h(\lambda) \equiv E(u + \lambda(v - u))$. When $\lambda = 0$, $h(\lambda)$ is minimized and hence $h'(0) \geq 0$. It follows that

$$h'(0) = \lim_{\lambda \rightarrow 0^+} \frac{1}{\lambda} \{E(u + \lambda(v - u)) - E(u)\} \geq 0. \quad (2.3)$$

Substituting (2.1) into (2.3), the solution $u \in K$ satisfies the elliptic variational inequality

$$\int_{\Omega} \nabla u \nabla(v - u) dx dy \geq \int_{\Omega} f(v - u) dx dy, \quad \forall v \in K. \quad (2.4)$$

Conversely, suppose u satisfies (2.4). Then for $\forall v \in K$,

$$\begin{aligned} E(v) &= E(u + (v - u)) \\ &= E(u) + \int_{\Omega} \nabla u \nabla(v - u) dx dy - \int_{\Omega} f(v - u) dx dy + \frac{1}{2} \int_{\Omega} |\nabla(v - u)|^2 \\ &\geq E(u) + \frac{1}{2} \int_{\Omega} |\nabla(v - u)|^2 \geq E(u), \end{aligned}$$

and hence u is also a solution of (2.1) (or (2.2)).

Linear complementarity formulation

Define two disjoint subsets of K such that $K = K_1 \cup K_2$ where

$$K_1 = \{u \in K : u = \psi\},$$

and

$$K_2 = \{u \in K : u > \psi\}.$$

Take an arbitrary $\phi \in K_2$. There exists $\epsilon_0 > 0$ such that $v = u \pm \epsilon\phi \in K$ for $0 < \epsilon \leq \epsilon_0$. Substituting $v = u \pm \epsilon\phi$ into (2.4), we have

$$\int_{\Omega} \nabla u \cdot \nabla(\pm\epsilon\phi) dx dy - \int_{\Omega} f(\pm\epsilon\phi) dx dy \geq 0. \quad (2.5)$$

Rearranging (2.5) and integrating by parts, we obtain

$$\pm\epsilon \int_{\Omega} (-\Delta u - f)\phi \geq 0, \quad \forall \phi \in K_2,$$

assuming $u \in C^2(\Omega)$. Since the inequality holds for both $+\epsilon$ and $-\epsilon$, it follows that

$$-\Delta u = f, \quad u(x, y) > \psi(x, y). \quad (2.6)$$

For the case in which $u(x, y)$ is not strictly greater than $\psi(x, y)$, let $\phi \in K$, and $\phi \geq 0$. Let $v = u + \phi \in K$. Then (2.4) becomes

$$\int_{\Omega} \nabla u \cdot \nabla \phi dX - \int_{\Omega} f \phi dX \geq 0.$$

Following a similar argument, we have

$$\int_{\Omega} (-\Delta u - f)\phi \geq 0,$$

for any $\phi \geq 0$. This implies that

$$-\Delta u - f \geq 0, \quad u(x, y) \geq \psi(x, y). \quad (2.7)$$

Combining the two cases (2.6) and (2.7), the obstacle problem can be written as a linear complementarity problem:

$$\begin{aligned} u - \psi &\geq 0, \\ -\Delta u - f &\geq 0, \\ (u - \psi)(-\Delta u - f) &= 0. \end{aligned} \quad (2.8)$$

HJB equation formulation

Equation (2.8) implies that if $u - \psi > 0$, then $-\Delta u - f = 0$. Otherwise, if $u - \psi = 0$, then $-\Delta u - f \geq 0$. Hence, the linear complementarity problem (2.8) can be written as

$$\min(-\Delta u - f, u - \psi) = 0, \quad \text{on } \Omega, \quad (2.9)$$

which is an HJB equation.

The above formulation is for the lower obstacle problem. For the upper obstacle problem, the equations can be derived similarly. In particular, the corresponding HJB equation is given by,

$$\max(-\Delta u - f, u - \psi) = 0, \quad \text{on } \Omega. \quad (2.10)$$

Here, $u \in K^{upper}$, where $K^{upper} = \{u \in H^1 | u \geq \psi\}$. For the two sided obstacle problem, the solution $u \in K^{two} \equiv \{u \in H^1 | \psi^1 \leq u \leq \psi^2\}$. The HJB equation is then given by

$$\max_{1 \leq \mu \leq 4} [-L^\mu u - f^\mu] = 0, \quad (2.11)$$

where

$$\begin{aligned} -L^\mu u &= [\text{sgn}(u - \psi^\mu)](-\Delta u), & f^\mu &= [\text{sgn}(u - \psi^\mu)]f, & \mu &= 1, 2, \\ -L^\mu u &= (-1)^\mu u, & f^\mu &= (-1)^\mu \psi^{\mu-2}, & \mu &= 3, 4. \end{aligned} \quad (2.12)$$

2.2. Minimal Surfaces with Obstacles

In the literature, another commonly studied obstacle problem is related to minimal surfaces. This model assumes that the potential energy due to the deformation of the membrane is proportional to the increase in the surface area, which is given by

$$\int_{\Omega} \sqrt{1 + |\nabla u|^2} dX, \quad u \in K. \quad (2.13)$$

The obstacle problem, similar to the minimal surface problem, is to find a solution $u \in K$ that minimizes the above potential energy:

$$\int_{\Omega} \sqrt{1 + |\nabla u|^2} dx dy \leq \int_{\Omega} \sqrt{1 + |\nabla v|^2} dx dy, \quad \forall v \in K. \quad (2.14)$$

We remark that the minimal surface obstacle problem is related to the previous model based on the linear theory of elasticity. Taking the Taylor's expansion of the integrand in (2.13), we have

$$\sqrt{1 + |\nabla u|^2} = 1 + \frac{1}{2} |\nabla u|^2 + O(|\nabla u|^4). \quad (2.15)$$

For small $|\nabla u|$, by dropping the higher order terms $O(|\nabla u|^4)$, the minimal surface obstacle problem becomes the elastic membrane constrained obstacle problem in (2.1).

Similar to the derivation in Section 2.1 which we have omitted here, (2.14) can be formulated as a variational inequality:

$$\int_{\Omega} \frac{\nabla u \cdot \nabla(v-u)}{\sqrt{1+|\nabla u|^2}} dx dy - \int_{\Omega} f(v-u) dx dy \geq 0, \quad \forall v \in K. \quad (2.16)$$

With a similar argument as in (2.6) and (2.7), one can show that u satisfies the following equations:

$$\begin{aligned} Au &\equiv -\nabla \cdot \left(\frac{\nabla u}{\sqrt{1+|\nabla u|^2}} \right) = f && \text{for } u(x, y) > \psi(x, y), \\ Au &\equiv -\nabla \cdot \left(\frac{\nabla u}{\sqrt{1+|\nabla u|^2}} \right) \geq f && \text{for } u(x, y) \geq \psi(x, y). \end{aligned} \quad (2.17)$$

This is similar to the linear complementarity formulation of the problem in (2.8).

The HJB equations for the minimal surface obstacle problem can be obtained by replacing the Δu and L^μ operators in (2.9), (2.10) and (2.11). More precisely, the equations for the lower and upper minimal surface obstacle problems are

$$\begin{aligned} \min(Au - f, u - \psi) &= 0, && \text{on } \Omega, \\ \max(Au - f, u - \psi) &= 0, && \text{on } \Omega, \end{aligned} \quad (2.18)$$

respectively. For the two sided minimal surface obstacle problem, the corresponding HJB equation is given by

$$\max_{1 \leq \mu \leq 4} [G^\mu u - f^\mu] = 0 \quad (2.19)$$

where

$$\begin{aligned} G^\mu u &= [\text{sgn}(u - \psi^\mu)](Au), & f^\mu &= [\text{sgn}(u - \psi^\mu)]f, & \mu &= 1, 2, \\ G^\mu u &= (-1)^\mu u, & f^\mu &= (-1)^\mu \psi^{\mu-2}, & \mu &= 3, 4. \end{aligned} \quad (2.20)$$

The term Au is defined in (2.17) for all these three HJB equations.

Remark: The minimal surface obstacle problem is similar to the elastic membrane constrained obstacle problem as shown above. The main difference lies on the operators in the model equations. In the elastic membrane obstacle problem, the Laplace operator Δ is linear and does not depend on the solution u . On the other hand, in the minimal surface obstacle problem, the operator A defined in (2.17) depends on u and is hence nonlinear. Nevertheless, we should also remark that both obstacle problems are nonlinear regardless of the differential operators due to the obstacle constraint.

2.3. Discretization of the Model HJB Equations

In this paper, we will primarily focus on the HJB formulation of the two obstacle problems defined on a unit square; i.e. $\Omega = (0, 1) \times (0, 1)$. We apply standard finite difference approximation to discretize the HJB equation in (2.9). Denote the grid points by (x_i, y_j) ,

where $x_i = i\Delta x$, $y_j = j\Delta y$, $0 \leq i, j \leq m+1$ with grid size $\Delta x = \Delta y = h = \frac{1}{m+1}$. Let $u_{i,j}$ be an approximation to $u(x_i, y_j)$. Then a finite difference discretization of the Laplace operator can be written as

$$-\frac{u_{i+1,j} - 2u_{i,j} + u_{i-1,j}}{h^2} - \frac{u_{i,j+1} - 2u_{i,j} + u_{i,j-1}}{h^2} = f_{i,j}, \quad 1 \leq i, j \leq m, \quad (2.21)$$

which will be denoted by the matrix A_h^{EM} of size $n \times n$, $n = m^2$. The superscript "EM" here refers to the elastic membrane constrained obstacle problem.

Similarly, we apply a finite difference method to discretize the operator in (2.17), which results in the following finite difference equations:

$$A_h^{MS} u_{i,j} = AC u_{i,j} + AW u_{i-1,j} + AE u_{i+1,j} + AS u_{i,j-1} + AN u_{i,j+1}. \quad (2.22)$$

The superscript "MS" in A_h^{MS} here refers to the minimal surface obstacle problem, and the weights AC , AW , AE , AS , AN are given by

$$AW = -\frac{1}{h^2} \left(\frac{1}{2\sqrt{\left(\frac{u_{i,j}-u_{i-1,j}}{h}\right)^2 + \left(\frac{u_{i,j}-u_{i,j-1}}{h}\right)^2 + 1}} + \frac{1}{2\sqrt{\left(\frac{u_{i,j}-u_{i-1,j}}{h}\right)^2 + \left(\frac{u_{i-1,j+1}-u_{i-1,j}}{h}\right)^2 + 1}} \right),$$

$$AE = -\frac{1}{h^2} \left(\frac{1}{2\sqrt{\left(\frac{u_{i+1,j}-u_{i,j}}{h}\right)^2 + \left(\frac{u_{i+1,j}-u_{i+1,j-1}}{h}\right)^2 + 1}} + \frac{1}{2\sqrt{\left(\frac{u_{i+1,j}-u_{i,j}}{h}\right)^2 + \left(\frac{u_{i,j+1}-u_{i,j}}{h}\right)^2 + 1}} \right),$$

$$AS = -\frac{1}{h^2} \left(\frac{1}{2\sqrt{\left(\frac{u_{i,j}-u_{i-1,j}}{h}\right)^2 + \left(\frac{u_{i,j}-u_{i,j-1}}{h}\right)^2 + 1}} + \frac{1}{2\sqrt{\left(\frac{u_{i+1,j-1}-u_{i,j-1}}{h}\right)^2 + \left(\frac{u_{i,j}-u_{i,j-1}}{h}\right)^2 + 1}} \right),$$

$$AN = -\frac{1}{h^2} \left(\frac{1}{2\sqrt{\left(\frac{u_{i+1,j}-u_{i,j}}{h}\right)^2 + \left(\frac{u_{i,j+1}-u_{i,j}}{h}\right)^2 + 1}} + \frac{1}{2\sqrt{\left(\frac{u_{i,j+1}-u_{i-1,j+1}}{h}\right)^2 + \left(\frac{u_{i,j+1}-u_{i,j}}{h}\right)^2 + 1}} \right),$$

and $AC = -(AW + AE + AS + AN) + 1$.

Let $u^h = [u_{1,1}, u_{2,1}, \dots, u_{m,m}]$ be the solution vector in the lexicographical ordering. The forcing vector f^h is defined similarly. Depending on the type of constraints, we divide the discrete obstacle problem into three types: (1) the lower obstacle, the set $K_h^L = \{v^h \in \mathbb{R}^n | v^h \geq \psi^{L,h}\}$, (2) the upper obstacle, the set $K_h^U = \{v^h \in \mathbb{R}^n | v^h \leq \psi^{U,h}\}$, (3) the two sided obstacle, $K_h^{two} = \{v^h \in \mathbb{R}^n | \psi^{L,h} \leq v^h \leq \psi^{U,h}\}$. Here $\psi^{L,h}$ and $\psi^{U,h}$ are the vectors of the discrete obstacle functions, and the inequalities are understood as componentwise. The discrete HJB equations are given as

$$\min[A_h(u^h) - f^h, u^h - \psi^{L,h}] = 0, \quad (2.23)$$

for the lower obstacle $K_h = K_h^L$,

$$\max[A_h(u^h) - f^h, u^h - \psi^{U,h}] = 0,$$

for the upper obstacle $K_h = K_h^U$, and

$$\max_{1 \leq \mu \leq 4} [A_h^\mu(u^h) - f^{\mu,h}] = 0,$$

for the two sided obstacle problem $K_h = K_h^{two}$, where

$$\begin{aligned} A_h^\mu(u^h) &= [\text{sgn}(u^h - \psi^{\mu,h})]A_h(u_h), & f^{\mu,h} &= [\text{sgn}(u^h - \psi^{\mu,h})]f^h, & \mu &= 1, 2, \\ A_h^\mu(u^h) &= (-1)^\mu u^h, & f^{\mu,h} &= (-1)^\mu \psi^{\mu-2,h}, & \mu &= 3, 4. \end{aligned}$$

For the above equations, $A_h = A_h^{EM}$, as defined in (2.21) for the elastic membrane constrained obstacle problem and $A_h = A_h^{MS}$, given by (2.22), for the minimal surface obstacle problem. We note again that the HJB equations should be understood componentwise.

In this paper, we will consider solving the discrete HJB equation with lower obstacle; i.e (2.23). As such, we simply denote the discrete obstacle function as ψ^h instead of $\psi^{L,h}$. The discrete HJB equation is difficult to solve numerically because of its nonlinearity. Whether a grid point is active or inactive depends on both $A_h(u^h)_i - f_i^h$ and $u_i^h - \psi_i^h$. However, we do not know that a priori. It in turn depends on the solution u^h and the obstacle function ψ^h . The minimal surface obstacle problem further complicates the problem where the operator A_h^{MS} itself is also nonlinear.

One approach to solve HJB equations in general is the policy iteration [1, 11, 14]. The policy iteration consists of an outer and inner loop. In the outer loop, it determines the active and inactive sets from the current approximate solution. In the inner loop, the active and inactive sets are held fixed which results in a linear system for the elastic membrane obstacle problem and a nonlinear system for the minimal surface obstacle problem. An iterative method may be used to solve the discrete problem in the inner loop. Since it involves outer and inner iterations, the total computational cost may be expensive in some cases.

3. Multigrid methods

In this paper, we will propose efficient multigrid methods based on the full approximate scheme (FAS) to solve nonlinear obstacle problems. Similar to the standard linear multigrid method, the FAS algorithm also consists of three major steps: pre-smoothing, coarse grid correction, and post-smoothing. Similar to a V-cycle, we only perform one coarse grid correction on each grid in our FAS. The problem on the coarsest grid is solved by the smoother. The components needed to be defined are the smoother, the interpolation and restriction operators, and the coarse grid operator.

3.1. Pre-Smoothing and Post-Smoothing

For the smoothing operator of the FAS, we propose the use of a modified version of the Newton-Gauss-Seidel (NGS) method. The Newton's method is a well known method for solving $\mathcal{F}(x) = 0$ [15] where $\mathcal{F} : \mathbb{R}^n \rightarrow \mathbb{R}^n$ is a continuously differentiable operator; i.e., a smooth operator and x is a vector in \mathbb{R}^n . The operator \mathcal{F} may depend on the vector x .

One step of the standard Newton's method is given by

$$x^{k+1} = x^k - \mathcal{F}'(x^k)^{-1} \mathcal{F}(x^k). \quad (3.1)$$

However, if \mathcal{F} is not a smooth operator but a locally Lipschitz operator, then (3.1) cannot be used anymore.

Let $\partial \mathcal{F}(x^k)$ be the generalized Jacobian of \mathcal{F} at x^k as defined in [4]. One can write (3.1) as

$$x^{k+1} = x^k - \mathcal{V}_k^{-1} \mathcal{F}(x^k), \quad (3.2)$$

where $\mathcal{V}_k \in \partial \mathcal{F}(x^k)$. The Newton's method extends to a non-smooth case by using the generalized Jacobian \mathcal{V}_k instead of the derivative $\mathcal{F}'(x^k)$ [18]. We can rewrite (3.2) as

$$\mathcal{V}_k x^{k+1} = \mathcal{V}_k x^k - \mathcal{F}(x^k). \quad (3.3)$$

It is shown that the local and global convergence results hold for (3.3) in [18] when \mathcal{F} is semismooth.

Solving the linear system (3.3) can be expensive. The NGS method that we are using as a smoother for our multigrid is to solve (3.3) approximately by Gauss-Seidel. In general, the NGS method we used here can be viewed as a non-smooth version of the standard NGS.

We first consider the case of the elastic membrane constrained obstacle problem. One iteration of the NGS smoother for the model problem consists of the following steps. Suppose the approximation \hat{u}_h^k after the k^{th} iteration of the NGS is known. Then we determine the active and inactive sets based on \hat{u}_h^k . More specifically, we construct the linearized equation for (2.23), which can be written as

$$N_h u^h = b^h. \quad (3.4)$$

The matrix N_h can be considered as the merging of the rows of two matrices. One matrix is A_h and the other is the identity matrix I_h with the same size as A_h . If a grid point with ordering i is active, which means $A_h(u^h)_i - f_i^h \geq u_i^h - \psi_i^h$, we take the i^{th} row from I_h . Meanwhile, we define the right hand side $b_i^h = \psi_i^h$. Otherwise, we take the i^{th} row from A_h and let $b_i^h = f_i^h$. To be more precise, the matrix N_h and the right hand side b^h are defined as

$$N_h(i, :) = \begin{cases} A_h(i, :), & \text{if the } i^{\text{th}} \text{ grid point is inactive,} \\ I_h(i, :), & \text{otherwise,} \end{cases} \quad (3.5)$$

$$b_i^h = \begin{cases} f_i^h, & \text{if the } i^{\text{th}} \text{ grid point is inactive,} \\ \psi_i^h, & \text{otherwise,} \end{cases} \quad (3.6)$$

where $(i, :)$ means the i^{th} row of a matrix. Finally, we apply one iteration of the Gauss-Seidel method to (3.4) to obtain \hat{u}_h^{k+1} .

For the case of the minimal surface obstacle problem, the operator A_h depends on the solution u^h . We further linearize it by fixing the entries of A_h by \hat{u}_h^k .

3.2. Restriction and Prolongation Operators

In standard FAS, the restriction operator is either injection and full weighting. We found that they both work well with full weighting performing slightly better. We will use full weighting for restricting both the residual and the solution to the coarse grid.

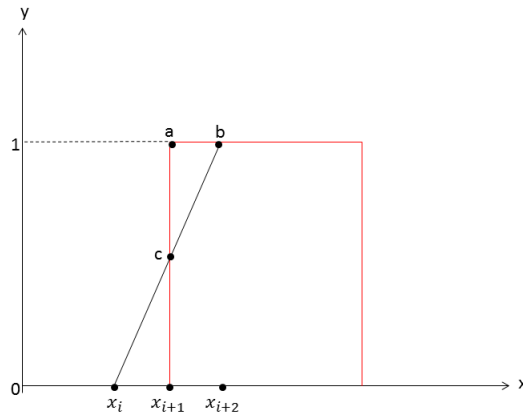


Figure 2: An illustration of the constraint preserving interpolation. The obstacle is represented by the solid (red) line. The constraint preserving interpolation gives a value of 1 (point a) while the standard linear interpolation would give a value between 0 and 1 (point c) at the noncoarse grid point x_{i+1} .

The bilinear interpolation operator is typically used as the prolongation operator in standard FAS. However, this operator is not working well for the obstacle problem. Figure 2 shows a 1D obstacle problem example which explains the drawback of the linear interpolation. In the figure, the grid points x_i and x_{i+2} are coarse grid points, and all x_i , x_{i+1} and x_{i+2} are points on the fine grid. The rectangle denotes the obstacle we are considering. Let \tilde{u}^H and \tilde{u}^h be the approximate solutions on the coarse grid and the fine grid, respectively. Suppose x_{i+1} and x_{i+2} are active points on the fine grid. So \tilde{u}_{i+1}^h and \tilde{u}_{i+2}^h should be equal to the obstacle value, which is 1 in our example. We also assume $\tilde{u}^H = 0$ at x_i . Using linear interpolation, we will have \tilde{u}_{i+1}^h equal to the value of c instead of 1, which is not accurate.

To address this issue, we modify the linear interpolation as follows. In the coarse grid correction step, when we update the fine grid solution using the interpolated error from

the coarse grid, we only do so at the inactive points; i.e. at the grid points where the solution is not constrained by the obstacle. We do not update the fine grid solution at the active points, thus preserving the obstacle values (assuming the initial guess satisfies the obstacle constraint). In this way, the modified interpolation will not create the problem as shown in Figure 2.

3.3. Nonlinear Operator N_H on Coarse Grid

3.3.1. N_H for Elastic Membrane Constrained Obstacle Problem

Direct discretization is typically used for the coarse grid operator in standard FAS. However, we observed that this coarse grid operator results in slow convergence. For linear PDE problems, the Galerkin coarse grid operator is also used which often yields fast multigrid convergence. Since the Laplacian operator in the elastic membrane constrained problem, i.e. A_h^{EM} in (2.23), is also linear, we can make use of the Galerkin coarse grid operator in the nonlinear problem here. This choice results in a faster convergence rate than the direct discretization.

We write the coarse grid HJB equation as

$$\min(A_H u^H, u^H - \psi^H) = \mathcal{R} \tilde{r}^h + N_H \mathcal{R} \tilde{u}^h, \quad (3.7)$$

where \mathcal{R} is the restriction operator, \tilde{u}^h is the approximate solution after pre-smoothing, and \tilde{r}^h is the residual of \tilde{u}^h . The right hand side of the coarse grid HJB equation comes from the standard FAS algorithm. For simplicity, the problem can be written as

$$N_H u^H = b^H, \quad (3.8)$$

where N_H is the matrix on the coarse grid. N_H is obtained from the merging of A_H and I_H (the identity matrix) in the same way as (3.5).

In order to compute the matrix N_H , we need to have A_H . Motivated by the Galerkin approach, we define the matrix $A_H = \mathcal{R} N_h \mathcal{P}$, where \mathcal{P} is the prolongation operator and N_h is the matrix on the fine grid. Note that we use N_h instead of A_h in order to define A_H . Thus we are applying the Galerkin method to the fine grid nonlinear operator.

The active and inactive points are the same as those on the fine grid. If an i^{th} point is active on the fine grid, then the left hand side of (3.8) becomes $N_H(u^H)_i = I_H(u^H)_i = u_i^H$ and the corresponding $b_i^H = (\psi^H + \mathcal{R} \tilde{r}^h + N_H \mathcal{R} \tilde{u}^h)_i$. Thus the equation becomes $u_i^H = (\psi^H + \mathcal{R} \tilde{r}^h + N_H \mathcal{R} \tilde{u}^h)_i$ at the i^{th} point. If the point is inactive, then the left hand side of (3.8) is $A_H(u^H)_i$, and we let $b_i^H = (\mathcal{R} \tilde{r}^h + N_H \mathcal{R} \tilde{u}^h)_i$. The equation reads $A_H(u_H)_i = (\mathcal{R} \tilde{r}^h + N_H \mathcal{R} \tilde{u}^h)_i$.

We can get a hierarchy of coarse grid operators by repeating the above process recursively. This forms a multigrid method. We remark that the operator we introduced is quite different from the direct discretization operator since the matrix A_H in the direct discretization is independent of N_h , but A_H in our method depends on N_h .

Since the Galerkin operator results in fast convergence for the elastic membrane constrained obstacle problem, it is natural to apply it to the minimal surface obstacle problem.

However, the Galerkin approach does not work well for the minimal surface obstacle problem.

The Galerkin process defines the coarse grid operator based merely on the fine grid operator. This does not cause any problem with the elastic membrane obstacle problem as the Laplacian operator A_h^{EM} in (2.21) is independent of the solution u^h . The coarse grid operator computed using the Galerkin approach will be just given by $A_H^{EM} = \mathcal{R}N_h\mathcal{P}$.

For the minimal surface obstacle problem, the fine grid operator A_h^{MS} in (2.22) depends on the solution u^h . It is desirable that the operator A_H^{MS} on the coarse grid would also depend on u^H . However, the Galerkin approach would give $A_H^{MS} = \mathcal{R}N_h\mathcal{P}$, which is independent of u^H (at least not directly). Thus the Galerkin coarse grid operator may not be effective for the minimal surface obstacle problem.

Instead, we utilize the direct discretization operator as the coarse grid operator. This operator on the coarse grid depends on u^H explicitly and it results in faster convergence.

4. Numerical Results

We will demonstrate the proposed V-cycle FAS scheme by solving 1D and 2D obstacle problems. Two pre-smoothing and post-smoothing steps are used. The stopping criterion for all the obstacle problems is that the norm of the residual of the problem at the inactive grid point is less than 10^{-6} . The obstacles considered in the numerical examples are a square obstacle (or block obstacle) and a circle obstacle (or dome obstacle); see Figure 3.

4.1. 1D Block Obstacle Problem with Laplacian Operator

We consider a 1D lower obstacle problem subject to a lower block obstacle:

$$u(x) \geq \psi(x) = \begin{cases} 1, & \frac{11}{32} \leq x \leq \frac{21}{32}, \\ 0, & \text{otherwise.} \end{cases} \quad (4.1)$$

Note that the obstacle is defined such that its boundary does not align with the coarse grids. In other words, the obstacle boundary on the coarse grids is off from the fine grid. Also, we note that the free boundary is actually known in this case (the given obstacle boundary) but our multigrid solver does not take advantage of this fact.

We apply the proposed V-cycle FAS to solve the HJB equation for the lower obstacle problem. Table 1 shows the FAS iteration numbers for different grid sizes and levels. We can see that the convergence is fast and is essentially independent of the grid size. Figure 4 shows the obstacle and the numerical solution of this 1D obstacle problem. We note that the free boundary coincides with the obstacle boundary.

4.2. 1D Dome Obstacle Problem with Laplacian Operator

The HJB equation of the 1D dome obstacle problem is similar to the 1D block obstacle except for the obstacle function. For the block obstacle, the elastic membrane will contact

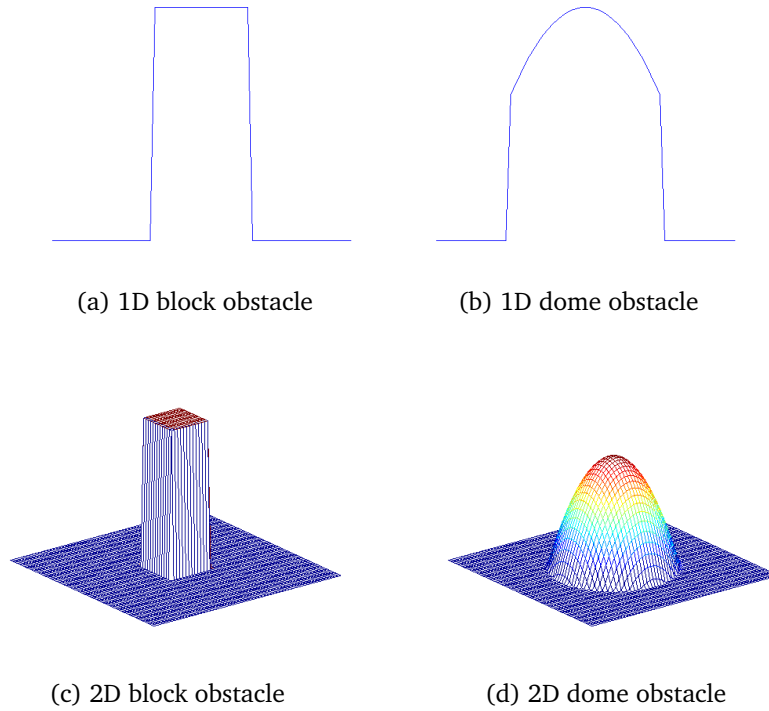


Figure 3: Pictures of different obstacles.

with the obstacle exactly on the surface of the obstacle. For the dome obstacle, it is not the case. Figure 5 (right) shows the difference between the numerical solution and the obstacle. We can see that the free boundary does not coincide with the obstacle boundary. Since the active set and inactive set depend on not only the shape of the dome obstacle but also the numerical solution, the obstacle problem with the dome obstacle is more difficult than the one with the block obstacle.

The problem we consider here is with the constraints:

$$u(x) \geq \psi(x) = \begin{cases} 1 - 6(x - 0.5)^2, & \frac{31}{128} \leq x \leq \frac{97}{128}, \\ 0, & \text{otherwise.} \end{cases} \quad (4.2)$$

Grid Size (h)	Levels	FAS Iterations
$\frac{1}{8}$	2	3
$\frac{1}{16}$	3	4
$\frac{1}{32}$	4	5
$\frac{1}{64}$	5	4
$\frac{1}{128}$	6	5

Table 1: Iterations of the FAS for the 1D block problem

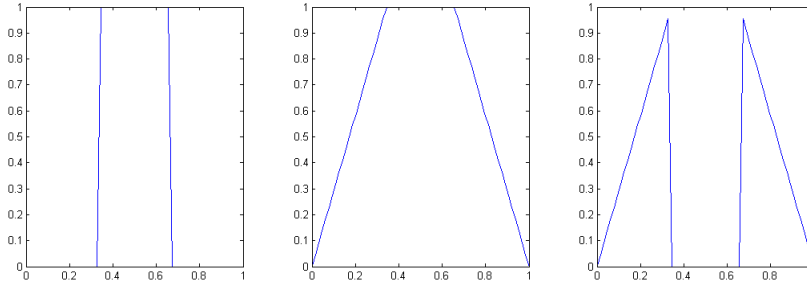


Figure 4: 1D block obstacle problem. (Left) obstacle, (middle) numerical solution, (right) difference between the obstacle and the numerical solution, with grid size $\frac{1}{64}$ and 5 levels.

Grid Size(h)	Levels	FAS Iterations
$\frac{1}{8}$	2	1
$\frac{1}{16}$	3	5
$\frac{1}{32}$	4	7
$\frac{1}{64}$	5	5
$\frac{1}{128}$	6	6

Table 2: Iterations of the FAS for the 1D dome problem.

The dome obstacle problem shares the same HJB equation with the previous example except that the obstacle function ψ is now given by (4.2). Using the V-cycle FAS, the iterations are given in Table 2. The obstacle, numerical solution, and the difference between the two are shown in Figure 5. The difference between the numerical solution and the obstacle indicates the contact parts between the obstacle and the solution.

Similar to Table 1, Table 2 shows that the iteration numbers of the FAS for solving the dome obstacle problem are independent of the grid size and the iteration numbers are about 5 to 6.

4.3. 2D Dome Obstacle Problem with Laplacian Operator

The 2D obstacle problem in this example is similar to the 1D dome obstacle. The obstacle function is given by:

$$u(x, y) \geq \psi(x, y) = \max\{0, 0.6 - 8|(x - 0.5)^2 + (y - 0.5)^2|\}. \quad (4.3)$$

The FAS iteration numbers are shown in Table 3. Figure 6 shows the obstacle, the solution and the difference for the 2D dome obstacle problem.

We will compare our method with the methods proposed in [13] and [17]. They both solve the elasto-plasto torsion problem which is similar to our numerical example here. The main difference is the shape of the obstacle. The obstacle considered in [13, 17] leaves the inactive set a small region with a cross shape aligned with two diagonals.

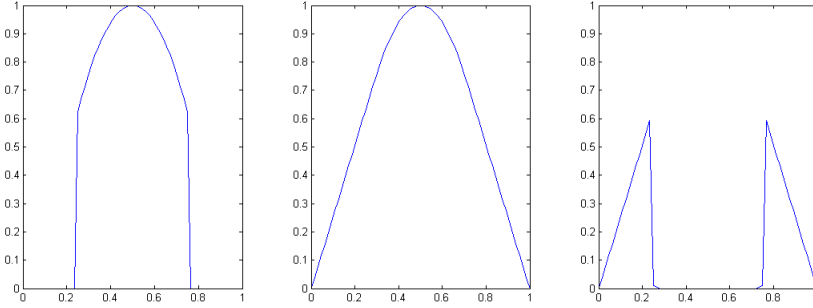


Figure 5: 1D Dome obstacle result. (Left) obstacle, (middle) numerical solution, (right) difference between the obstacle and the numerical solution, with grid size $\frac{1}{64}$ and 5 levels.

Grid Size(h)	Levels	FAS Iterations
$\frac{1}{8}$	2	5
$\frac{1}{16}$	3	5
$\frac{1}{32}$	4	6
$\frac{1}{64}$	5	7
$\frac{1}{128}$	6	9

Table 3: Iterations of the FAS for the 2D dome problem.

In [13], finite element methods are used as the discretization method and monotone multigrid methods are applied. To compare our method with the results reported in [13], we consider the iteration error computed as $\epsilon_h^k = \bar{u}_h - \hat{u}_h^k$, where \hat{u}_h^k is the approximate solution after k iterations and \bar{u}_h is the “exact” numerical solution computed with a small tolerance of 10^{-9} . The iteration numbers to achieve the same errors by our method and the TRCKH method in [13] are shown in Table 4. Our FAS method takes about half of the iterations of the TRCKH method to achieve the same errors. Since V-cycle is used by both the TRCKH and our FAS methods, the work per iteration is equivalent. It shows that our multigrid method has faster convergence.

In [17], a F-cycle multigrid is used to solve the obstacle problem. In order to compare the results in [17], we show here the rate of convergence for their F-cycle multigrid and our FAS multigrid in Table 5. For the two grid sizes reported, our proposed multigrid method has a faster convergence rate than the F-cycle multigrid. In addition, since the V-cycle is used in our FAS method, the work is less per iteration than the F-cycle multigrid.

4.4. 2D Dome Obstacle Problem with Minimal Surface Operator

Now, we consider an obstacle problem with the minimal surface operator. The obstacle considered here is the same as the 2D obstacle problem with the Laplacian operator (4.3). Convergence results for solving the corresponding HJB equations with the V-cycle FAS

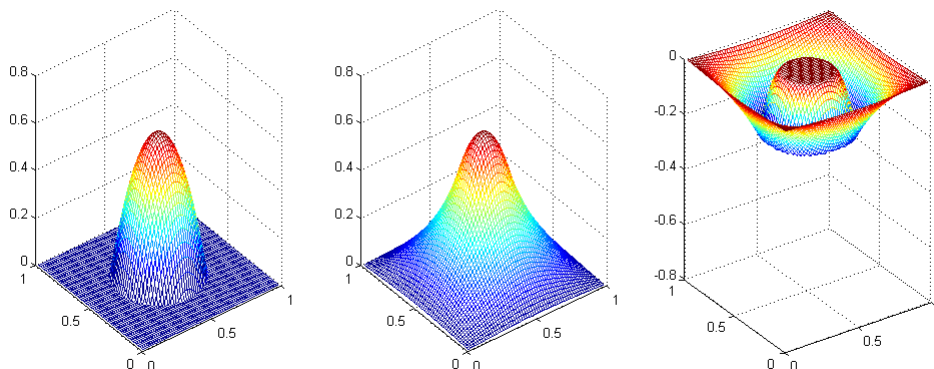


Figure 6: 2D dome obstacle result. (Left) obstacle, (middle) numerical solution, (right) difference between numerical solution and obstacle, with grid size $\frac{1}{64}$ and 5 levels.

Iteration Errors	10^{-2}	10^{-4}	10^{-6}	10^{-7}	10^{-8}
Number of Iterations for TRCKH	10	19	23	25	28
Number of Iterations for FAS	8	10	11	12	13

Table 4: Convergence of the TRCKH [13] and the proposed FAS multigrid methods.

algorithm are given in Table 6. Figure 7 shows the obstacle, the numerical solution, and the difference between them.

Table 7 shows the residuals for grid sizes $h = \frac{1}{16}$ and $h = \frac{1}{32}$ in each iteration computed by our FAS. For comparison, we have listed the residuals reported in [8] and [10]. It is noticed that the residuals given by the multigrid methods in [8] and [10] seem to converge faster to zero than the residuals given by the FAS method. However, a W-cycle is used in both methods. Considering the work in each W-cycle is about 1.5 times of that in one V-cycle, the total computational work of 9 iterations of our FAS, for instance, is about the same as 6 iterations of the W-cycle. From the table, we see that at the 9th iteration of our method, the residual is reduced to 8×10^{-9} (for the grid size $\frac{1}{16}$). However, for the other two methods, the residual after the 6th iteration is reduced to 2.2×10^{-7} and 5.9×10^{-7} , respectively.

A multigrid-type method based on subspace correction is proposed in [20] to solve a minimal surface obstacle problem. We note that the numerical experiment given in [20] is not exactly the same. A slightly different obstacle on the domain $\Omega = (-2, 2)^2$ is

	F-cycle	FAS
$h = \frac{1}{128}$	0.20	0.098
$h = \frac{1}{256}$	0.37	0.186

Table 5: Convergence of the F-cycle [17] and the proposed FAS multigrid methods.

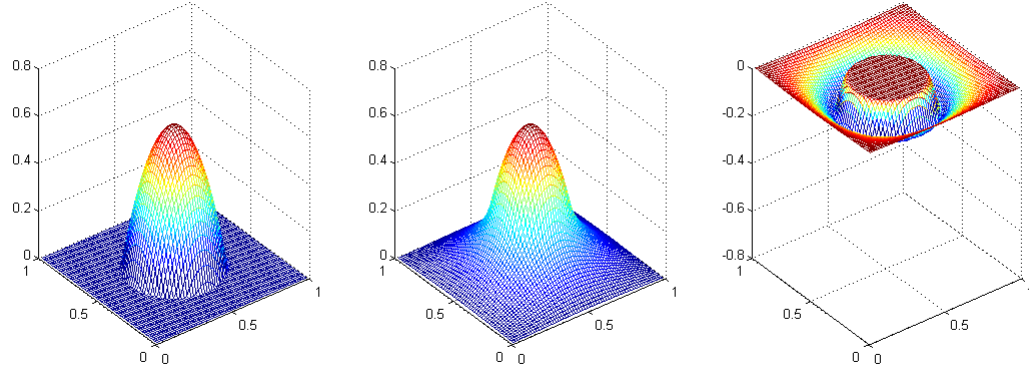


Figure 7: 2D dome obstacle with minimal surface operator. (Left) obstacle, (middle) numerical solution, (right) difference between the numerical solution and the obstacle, with grid size $\frac{1}{64}$ and 5 levels.

Grid Size(h)	Levels	FAS Iterations
$\frac{1}{8}$	2	4
$\frac{1}{16}$	3	6
$\frac{1}{32}$	4	11
$\frac{1}{64}$	5	10
$\frac{1}{128}$	6	15

Table 6: Iterations of the FAS for 2D dome problem with the minimal surface operator.

considered, but with a quite similar shape. Table 8 presents the convergence rates for the proposed FAS method and the subspace correction method. In the table, J is the number of coarse levels. The proposed FAS shows faster convergence.

5. Conclusion

In this paper, we have proposed a multigrid method based on the full approximate scheme for solving two types of obstacle problems using the HJB equation formulation. The Galerkin operator was often used as a coarse grid operator for linear problems. Here, we have proposed a special coarse grid operator based on the Galerkin approach for solving the elastic membrane constrained obstacle problem. This choice of coarse grid operator has improved the convergence of the FAS. For the minimal surface obstacle problem, we applied the direct discretization as the coarse grid operator. In addition, we have proposed a modified linear interpolation operator to address the issue of inaccurate prolongation near the boundary between the active and inactive sets. Numerical results show that our FAS converges in small numbers of iterations for the two model obstacle problems in 1D and 2D. Also, the proposed FAS multigrid compares favourably with other multigrid methods

Iteration	FAS	FAS	vimII	vimII	mgm	mgm
	$h = 1/16$	$h = 1/32$	$h = 1/16$	$h = 1/32$	$h = 1/16$	$h = 1/32$
1	1.6E - 2	3.7E - 2				
2	1.7E - 3	4.1E - 3			1.9E - 2	
3	2.4E - 4	8.2E - 4	2.4E - 4		1.3E - 3	1.1E - 3
4	3.7E - 5	3.1E - 4	2.3E - 5	1.1E - 3	9.4E - 5	3.6E - 4
5	5.9E - 6	1.2E - 4	2.2E - 6	4.2E - 4	7.2E - 6	1.4E - 4
6	9.7E - 7	4.9E - 5	2.2E - 7	1.5E - 4	5.9E - 7	5.6E - 5
7	1.7E - 7	2.0E - 5	2.0E - 8	5.3E - 5	5.3E - 8	2.3E - 5
8	3.6E - 8	8.1E - 6	5.0E - 9	1.9E - 5		
9	8.0E - 9	3.3E - 6	1.3E - 9	6.7E - 6		
10	1.9E - 9	1.4E - 6	3.2E - 10	2.4E - 6		

Table 7: Norms of residuals at each iteration given by the proposed FAS, vimII [10], and mgm [8] methods.

	J = 5	J = 6	J = 7	J = 8	FAS
Convergence Rate	0.78	0.8	0.81	0.85	0.40

Table 8: Convergence rates for the subspace correction method in [20] (columns 2 to 5) and the FAS (last column).

in the literature.

References

- [1] R.E. Bellman. *Introduction to the Mathematical Theory of Control Processes: Nonlinear processes*. Mathematics in science and engineering. Academic Press, 1971.
- [2] Achi Brandt and Colin W Cryer. Multigrid algorithms for the solution of linear complementarity problems arising from free boundary problems. *SIAM journal on scientific and statistical computing*, 4(4):655–684, 1983.
- [3] Luis A Caffarelli. The obstacle problem revisited. *Journal of Fourier Analysis and Applications*, 4(4):383–402, 1998.
- [4] F Clarke. *Optimization and nonsmooth analysis* wiley. New York, 1983.
- [5] Isabel Narra Figueiredo, José Francisco Rodrigues, and Lisa Santos. *Free Boundary Problems: Theory and Applications*, volume 154. Springer, 2007.
- [6] R Glowinski, Jacques Louis Lions, and Raymond Trémolières. *Numerical analysis of variational inequalities*, 1981.
- [7] Roland Glowinski. *Lectures on Numerical Methods for Non-Linear Variational Problems*. Springer, 2008.
- [8] Wolfgang Hackbusch and Hans Detlef Mittelmann. On multi-grid methods for variational inequalities. *Numerische Mathematik*, 42(1):65–76, 1983.
- [9] Michael Hintermüller and Karl Kunisch. Path-following methods for a class of constrained minimization problems in function space. *SIAM J. Optim.*, 17(1):159–187, 2006.

- [10] Ronald H.W. Hoppe. Multigrid algorithms for variational inequalities. *SIAM journal on numerical analysis*, 24(5):1046–1065, 1987.
- [11] Ronald A. Howard. *Dynamic Programming and Markov Process*. MIT Press, Cambridge, MA, USA, 1960.
- [12] Kazufumi Ito and Karl Kunisch. Semi-smooth Newton methods for variational inequalities of the first kind. *Mathematical Modelling and Numerical Analysis*, 37(1):41–62, 2003.
- [13] Ralf Kornhuber. Monotone multigrid methods for elliptic variational inequalities I. *Numerische Mathematik*, 69:167–167, 1994.
- [14] P-L. Lions and B. Mercier. Approximation numerique des equations Hamilton-Jacobi-Bellman. *RAIRO - Analyse numerique*, 14(4):369–393, 1980.
- [15] Jorge J Moré. Global convergence of newton-gauss-seidel methods. *SIAM Journal on Numerical Analysis*, 8(2):325–336, 1971.
- [16] Dianne P O’Leary. Conjugate gradient algorithms in the solution of optimization problems for nonlinear elliptic partial differential equations. *Computing*, 22(1):59–77, 1979.
- [17] Cornelis W Oosterlee. On multigrid for linear complementarity problems with application to American-style options. *Electronic Transactions on Numerical Analysis*, 15(165-185):2–7, 2003.
- [18] Liqun Qi and Jie Sun. A nonsmooth version of Newton’s method. *Mathematical programming*, 58(1-3):353–367, 1993.
- [19] J-F Rodrigues. *Obstacle problems in mathematical physics*, volume 134. North Holland, 1987.
- [20] Xue-Cheng Tai. Rate of convergence for some constraint decomposition methods for nonlinear variational inequalities. *Numerische Mathematik*, 93(4):755–786, 2003.